

1 ***HisCl1* regulates gustatory habituation in sweet taste neurons and mediates sugar ingestion**  
2 ***in Drosophila*.**

3

4 Haein Kim<sup>1</sup>, Ziqing Zhong<sup>1,2</sup>, Xinyue Cui<sup>1</sup>, Hayeon Sung<sup>3</sup>, Naman Agrawal<sup>1</sup>, Tianxing Jiang<sup>1</sup>, Monica  
5 Dus<sup>3</sup>, Nilay Yapici<sup>1,\*</sup>

6

7 <sup>1</sup> Department of Neurobiology and Behavior, Cornell University, Ithaca, NY, USA

8 <sup>2</sup> Current address: Tianqiao and Chrissy Chen Institute for Neuroscience, California Institute of  
9 Technology, Pasadena, CA, USA

10 <sup>3</sup> Department of Molecular, Cellular and Developmental Biology, The University of Michigan, Ann  
11 Arbor, MI, USA

12

13

14 \*Lead contact: Nilay Yapici ([ny96@cornell.edu](mailto:ny96@cornell.edu))

15

16

17

18 **SUMMARY**

19 Similar to other animals, the fly, *Drosophila melanogaster*, reduces its responsiveness to tastants with  
20 repeated exposure, a phenomenon called gustatory habituation. Previous studies have focused on  
21 the circuit basis of gustatory habituation in the fly chemosensory system <sup>1,2</sup>. However, gustatory  
22 neurons reduce their firing rate during repeated stimulation <sup>3</sup>, suggesting that cell-autonomous  
23 mechanisms also contribute to habituation. Here, we used deep learning-based pose estimation and  
24 optogenetic stimulation to demonstrate that continuous activation of sweet taste neurons causes  
25 gustatory habituation in flies. We conducted a transgenic RNAi screen to identify genes involved in  
26 this process and found that knocking down *Histamine-gated chloride channel subunit 1* (*HisCl1*) in  
27 the sweet taste neurons significantly reduced gustatory habituation. Anatomical analysis showed that  
28 *HisCl1* is expressed in the sweet taste neurons of various chemosensory organs. Using single sensilla  
29 electrophysiology, we showed that sweet taste neurons reduced their firing rate with prolonged  
30 exposure to sucrose. Knocking down *HisCl1* in sweet taste neurons suppressed gustatory habituation  
31 by reducing the spike frequency adaptation observed in these neurons during high-concentration  
32 sucrose stimulation. Finally, we showed that flies lacking *HisCl1* in sweet taste neurons increased  
33 their consumption of high-concentration sucrose solution at their first meal bout compared to control  
34 flies. Together, our results demonstrate that *HisCl1* tunes spike frequency adaptation in sweet taste  
35 neurons and contributes to gustatory habituation and food intake regulation in flies. Since *HisCl1* is  
36 highly conserved across many dipteran and hymenopteran species, our findings open a new direction  
37 in studying insect gustatory habituation.

38 **RESULTS**

39 ***HisC11* regulates gustatory habituation in sweet taste neurons**

40 The sense of taste allows animals to detect specific nutrients and avoid toxic compounds. The  
41 gustatory assessment of food is mainly regulated by the chemosensory neurons located in various  
42 taste organs<sup>4-6</sup>. The fly, *Drosophila melanogaster*, can assess food quality via taste neurons located  
43 in the proboscis, legs, and wings<sup>7-13</sup>. Stimulating sweet taste neurons in the labellum or legs triggers  
44 proboscis extension, followed by labellar opening and food ingestion<sup>14-17</sup>. Taste neurons can alter  
45 their activity based on the metabolic state or when exposed continuously to a particular nutrient<sup>18,19</sup>.  
46 For example, sweet taste neurons reduce their responsivity to sugars when flies are kept on a high-  
47 sugar diet<sup>20</sup>. These neurons also reduce their firing rate during prolonged sugar stimulation (Figures  
48 S1A and S1B), leading to a decrease in the proboscis extension response, a phenomenon called  
49 gustatory habituation<sup>3</sup>. Previous studies have focused on the circuit basis of gustatory habituation in  
50 flies<sup>2,18,19,21</sup>. Here we investigated the cell-intrinsic factors that allow sweet taste neurons to adapt to  
51 prolonged sensory stimuli.

52 To study gustatory habituation, we stimulated sweet taste neurons using a red-shifted  
53 channelrhodopsin, Chrimson, in hungry flies walking on an air-suspended spherical treadmill (Figure  
54 1A). In these experiments, we chose to use optogenetic activation instead of sugar stimulation to  
55 minimize the effects of satiation upon sugar ingestion on the fly's gustatory responsiveness. To  
56 automatically track the movements of the proboscis, we used DeepLabCut<sup>TM</sup>, a deep learning-based  
57 pose estimation software<sup>22</sup>. We used the coordinates of the head, rostrum, and haustellum to  
58 calculate the angle of the rostrum ( $\theta$ ) and used this metric to quantify gustatory habituation (Figures  
59 1B and 1C). During the continuous activation (total duration=60s, constant LED) of sweet taste  
60 neurons (*Gr64f>Chrimson*), flies extended their proboscis, but this response was quickly abolished  
61 within seconds (Figure 1D and Video S1). In contrast, when sweet taste neurons were transiently  
62 activated (total duration=60s, 0.1Hz pulsed LED), flies extended their proboscis consistently upon  
63 each LED stimulus onset without showing any signs of habituation (Figure 1E and Video S2). These  
64 results confirmed that continuous activation of sweet taste neurons indeed leads to gustatory  
65 habituation.

66 To identify cell-intrinsic factors regulating gustatory habituation in flies, we conducted a  
67 transgenic RNAi screen by knocking down specific genes in sweet taste neurons during continuous  
68 optogenetic activation. In the mammalian brain,  $\text{Ca}^{2+}$ -activated  $\text{Cl}^-$  channels (CACC) contribute to  
69 spike-frequency adaptation seen in the thalamocortical and hippocampal neurons<sup>23</sup>. We  
70 hypothesized that a similar spike frequency adaptation mechanism might mediate gustatory  
71 habituation in the fly sweet taste neurons. To test our hypothesis, we first searched for chloride  
72 channel genes expressed in the fly proboscis using previously published RNA sequencing datasets

73 <sup>20</sup>. Next, using transgenic RNAi, we knocked down chloride channel genes (n=14) in the sweet taste  
74 neurons and tested these mutant flies in optogenetic activation experiments, identifying two genes,  
75 *HisCl1* and *Clc-a*, as candidate regulators of gustatory habituation (Figure 2A and Figure S1C).  
76 *Gr64f>HisCl1-RNAi* and *Gr64f>Clc-a-RNAi* flies consistently exhibited reduced gustatory habituation  
77 during optogenetic activation (Figures 1C and 2B). *Gr64f>HisCl1-RNAi* induced the most significant  
78 suppression in gustatory habituation; these flies continued to extend their proboscis despite  
79 continuous stimulation of sweet taste neurons (Figure 2C and Video S3). To confirm the RNAi  
80 knockdown results, we tested *HisCl1* null mutants (*HisCl1*<sup>-/-</sup>). When sweet taste neurons were  
81 continuously activated in *HisCl1*<sup>-/-</sup> mutants, these flies showed a robust suppression in gustatory  
82 habituation similar to *Gr64f>HisCl1-RNAi* flies (Figures 1E and 2D). Interestingly, flies heterozygous  
83 for *HisCl1* (*HisCl1*<sup>+/+</sup>) behaved like hypomorphs; their gustatory habituation was not significantly  
84 different from *HisCl1*<sup>-/-</sup> mutants or controls (Figure 2E).

85 *HisCl1* gene encodes a histamine-gated chloride channel in flies. Two histamine-gated  
86 chloride channel genes are found in the *Drosophila* genome, *HisCl1* and *Ora transientless* (*Ort*)<sup>24-26</sup>.  
87 *HisCl1* and *Ort* work together in the fly visual system to mediate the inhibition between R7 and R8  
88 photoreceptors<sup>27</sup>. We hypothesized that *Ort* could also regulate gustatory habituation in sweet taste  
89 neurons similar to *HisCl1*. However, knocking down *Ort* did not impact gustatory habituation during  
90 the continuous activation of sweet taste neurons (Figures S2A and S2B). Consistent with our  
91 behavioral results, we found that GAL4 knock-in to the *Ort* gene (*Ort*>) did not label neurons in the fly  
92 chemosensory organs, while many optic lobe neurons were labeled in these flies (Figure S2C). Our  
93 results demonstrated that *HisCl1*, but not *Ort*, modulates gustatory habituation in sweet taste neurons.

94 **HisCl1 suppresses spike frequency adaptation in sweet taste neurons during high-  
95 concentration sugar stimulation**

96 To further investigate how *HisCl1* regulates gustatory habituation, we first examined its expression  
97 pattern in the fly taste organs. Using a GAL4 knock-in (*HisCl1*>), we found that *HisCl1* is broadly  
98 expressed in the labellum (Figure 3A). Our detailed anatomical characterization showed that *HisCl1*>  
99 labeled a subpopulation of sweet taste neurons expressing the sugar receptor *Gr64f*<sup>17,28</sup>. We  
100 observed  $5.5 \pm 0.5$  neurons that are co-labeled by *HisCl1*> and *Gr64f*> in the labellum (n=6),  $1.25 \pm$   
101 0.48 in the labral sense organ (LSO) (n=4), and  $0.5 \pm 0.29$  in the front tarsi (n=4) (Figure 3B). These  
102 results suggest that *HisCl1*<sup>+</sup> and *Gr64f*<sup>+</sup> cells contribute to gustatory habituation during continuous  
103 stimulation of sweet taste neurons.

104 In flies, gustatory habituation is thought to be regulated by changes in the activity of taste  
105 circuits, mainly arising from postsynaptic partners of taste neurons<sup>1,2</sup>. However, sweet taste neurons  
106 also adapt their firing rate during continuous optogenetic stimulation<sup>3</sup> or during prolonged sugar  
107 exposure (Figures S1A and S1B), suggesting there should be changes in the intrinsic properties of

108 these neurons leading to a depression in the firing rate. We hypothesize that HisCl1 might regulate  
109 gustatory habituation by directly altering sweet taste neuron firing rate during continuous stimulation.  
110 To directly test our hypothesis, we recorded the activity of HisCl1+ and Gr64f+ neurons located in the  
111 L4 sensillum in response to prolonged sucrose stimulation (Figure 3C). When the L4 sensillum was  
112 stimulated with 500mM sucrose, sweet taste neurons in both *Gr64f>HisCl1-RNAi* and control flies  
113 responded with a high initial firing rate that decreased within seconds, reaching a steady baseline  
114 (Figures 3C-3E). The firing rates reached a maximum between 0-1s after stimulus onset (Figures 3C  
115 and 3D). As we expected, the adaptation in firing rate was slower in *Gr64f>HisCl1-RNAi* flies  
116 compared to controls (Figures 3C and 3D, Figures S3C and 3D). To better quantify the temporal  
117 dynamics of neural activity during sugar stimulation, we compared the firing rates at early (0s≤t<1s),  
118 mid (10s≤t<11s and 30s≤t<31s), and late stages (50s≤t<51s) of the experiment (Figure 3D). The  
119 firing rates of sweet taste neurons in *Gr64f>HisCl1-RNAi* and control flies were not significantly  
120 different during the early or late stages of the sugar stimulation (Figures 3D, 3F, and 3I). However,  
121 during the mid-stages, while control flies rapidly adapted their firing rate after stimulus onset,  
122 *Gr64f>HisCl1-RNAi* flies continued to respond to the sugar stimulus with significantly higher firing  
123 rates (Figures 3D, 3G, and 3H). Interestingly, when we repeated the same experiment with 100mM  
124 sucrose solution, we found no differences in the firing rates of sweet taste neurons between the  
125 *Gr64f>HisCl1-RNAi* and control flies (Figures S3A and S3B). These results suggest that HisCl1  
126 regulates spike frequency adaptation in sweet taste neurons, specifically during high-concentration  
127 sugar stimulation.

## 128 HisCl1 is required in sweet taste neurons to regulate high-concentration sugar ingestion

129 Having established that HisCl1 regulates gustatory habituation and spike frequency adaptation in  
130 sweet taste neurons, we next explored how this behavioral and physiological adaptation impacts food  
131 intake behavior in flies. To quantify the temporal dynamics of food ingestion in *Gr64f>HisCl1-RNAi*  
132 and control flies, we used the Expresso automated food intake assay to capture meal-bouts of  
133 individual flies in real-time <sup>29</sup>. We provided different concentrations of sucrose solution (20mM,  
134 100mM, and 500mM) to 19-23hr food-deprived flies and recorded their ingestion behavior for 30  
135 minutes (Figures 4A-4C). Our results showed that *Gr64f>HisCl1-RNAi* flies consumed significantly  
136 higher amounts of 500mM sucrose in their first meal bout compared to controls, while there were no  
137 differences in other concentrations tested between *Gr64f>HisCl1-RNAi* and control flies (Figures 4D-  
138 4F). We repeated the same experiment for *HisCl1*<sup>-/-</sup> mutants and their genetic controls and found  
139 similar results (Figures S4A and S4B): *HisCl1*<sup>-/-</sup> mutants consumed higher amounts of 500mM sucrose  
140 in their first meal bout compared to control flies (Figure S4C), and this difference in the meal bout  
141 volume was not observed for flies tested with 100mM sucrose (Figure S4C). In these experiments,  
142 we also quantified the total volume ingested for each genotype and found no significant differences  
143 among the groups tested (Figure 4G and Figure S4D). Our results demonstrate that HisCl1 function

144 is required in sweet taste neurons to regulate meal bout volume when flies consume high  
145 concentration sucrose. Our findings from optogenetic activation, single sensillum recording, and food  
146 intake experiments led us to conclude that HisCl1 function is required in sweet taste neurons to  
147 suppress excessive sugar intake by fine-tuning spike frequency adaptation in these neurons.

148 **DISCUSSION**

149 Gustatory habituation and dishabituation have been studied in *Drosophila* in the context of  
150 learning/memory and on the level of neural circuits <sup>1</sup>. Here, we explored the cell-intrinsic mechanisms  
151 that regulate gustatory habituation in sweet taste neurons. We found a novel function for the  
152 histamine-gated chloride channel, HisCl1, in regulating temporal dynamics of sugar ingestion in  
153 hungry flies by fine-tuning the activity of sweet taste neurons. Interestingly, knocking down *HisCl1* in  
154 sweet taste neurons specifically suppressed gustatory habituation in response to high-concentration  
155 sucrose stimulation suggesting other cell-intrinsic factors also contribute to spike frequency  
156 adaptation in sweet taste neurons. Recently, it has been shown that a high-sugar diet decreases the  
157 stimulus-evoked firing rate and calcium responses of sweet taste neurons in flies due to the elevated  
158 activity of a conserved sugar sensor, O-linked N-Acetylglucosamine transferase (OGT) <sup>20</sup>. It is  
159 possible that HisCl1 and OGT work together or in parallel pathways to fine-tune the activity of sweet  
160 taste neurons. Moreover, HisCl1 is expressed in a subpopulation of taste neurons, indicating there  
161 might be other cell-intrinsic factors regulating gustatory habituation. For example, in our genetic  
162 screen, we also identified another chloride channel, *C/c-a*, as a putative regulator of gustatory  
163 habituation. Our results suggest that distinct chloride channels might finetune the activity of different  
164 classes of taste neurons in flies.

165 How does HisCl1 regulate spike frequency adaptation in sweet taste neurons? In the  
166 mammalian brain, spike frequency adaption is regulated by  $\text{Ca}^{2+}$ -activated chloride channels (CACC)  
167 <sup>23</sup>. When neurons are strongly activated, an increase in the local  $\text{Ca}^{2+}$  levels activate CACC, leading  
168 to an influx of  $\text{Cl}^-$  and hyperpolarization of membrane potential, thereby decreasing the probability of  
169 spike generation <sup>30</sup>. In the taste neurons of *Necturus*, an aquatic salamander,  $\text{Ca}^{2+}$ -dependent  $\text{Cl}^-$   
170 currents contribute to gustatory habituation <sup>31</sup>. It is unclear if such  $\text{Ca}^{2+}$ -dependent mechanisms trigger  
171 HisCl1 activation in the fly sweet taste neurons. Alternatively, HisCl1 might regulate gustatory  
172 habituation by changing synaptic release at the sweet taste neuron terminals. In the photoreceptors,  
173 HisCl1 plays a role in circadian entrainment via histamine signaling <sup>32,33</sup>. Likewise, sugar exposure  
174 might trigger histamine release in downstream circuits, which activate HisCl1 in the sweet taste  
175 neuron axon terminals leading to presynaptic depression and spike frequency adaptation. Such  
176 phenomenon of self-backpropagation of presynaptic depression has been previously reported in  
177 hippocampal neurons<sup>34,35</sup>. To discriminate between these two possibilities, one needs to determine  
178 the subcellular localization of HisCl1 in sweet taste neurons and characterize its Cl-channel properties

179 in response to the changes in intracellular  $\text{Ca}^{2+}$ . Future experiments will address these open  
180 questions.

181 Our study also found that HisCl1 mutants increase their meal bout volume when ingesting a  
182 high-concentration sugar solution. We speculate that the increase in meal bout volume is mediated  
183 by the reduction in sensory adaptation in sweet taste neurons; when sweet taste neurons cannot  
184 reduce their firing rate during prolonged exposure to sugar, flies cannot cease ingestion leading to an  
185 increase in the meal bout volume. These findings suggest that one function of gustatory habituation  
186 in flies might be to avoid excessive sugar intake. Interestingly, HisCl1 is conserved across many  
187 dipteran and hymenopteran species, suggesting similar mechanisms might exist for regulating food  
188 ingestion in other insect species, including agricultural pests and human disease vectors. Overall, our  
189 study opens a new direction to studying the cell-intrinsic factors that regulate gustatory habituation in  
190 flies. We think this is a step forward in understanding how the insects adapt their behavior and sensory  
191 physiology when faced with persistent sensory stimuli.

192

### 193 **ACKNOWLEDGEMENTS**

194 We thank the Yapici Lab members for their comments on the manuscript and Dr. David Anderson  
195 and Dr. Hubert Amrein for fly stocks. We acknowledge Bloomington Drosophila Stock Center (NIH  
196 P40OD018537) and the Developmental Studies Hybridoma Bank (NICHD of the NIH, University of  
197 Iowa) for reagents. Imaging data were acquired through the Cornell University Biotechnology  
198 Resource Center, with NIH S10OD018516 funding for the shared Zeiss LSM880 confocal/multiphoton  
199 microscope. Research in N.Y.'s lab is supported by a Pew Biomedical Scholar Award, the Alfred P.  
200 Sloan Foundation Award, and an NIH-R35-MIRA (R35GM133698). Research in M.D.'s lab is  
201 supported by a Klingenstein-Simons Fellowship in the Neurosciences, a Rita Allen Foundation  
202 Scholars award, and an NSF CAREER award (1941822).

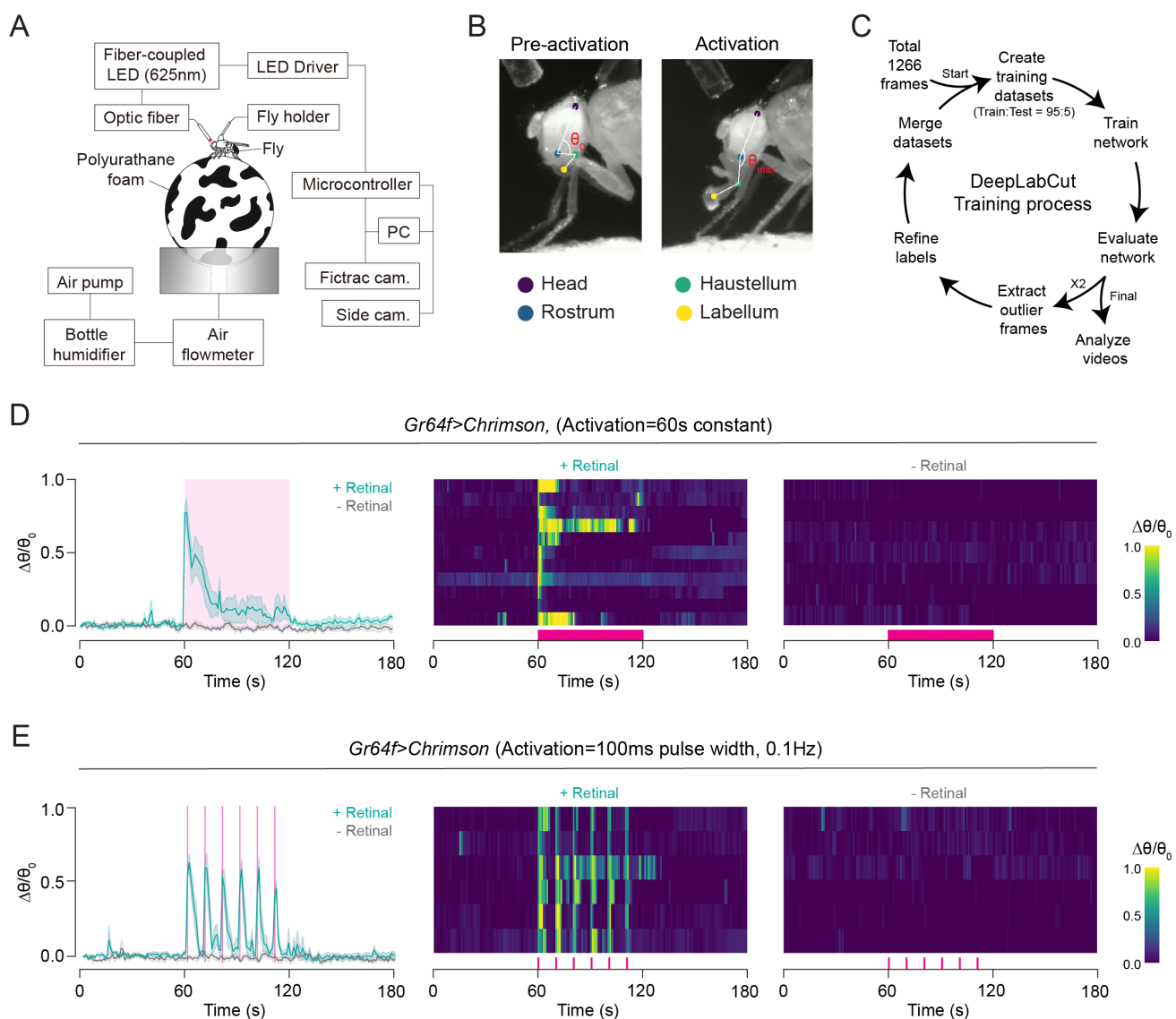
### 203 **AUTHOR CONTRIBUTIONS**

204 N.Y. and H.K. conceived the project and designed all the experiments. H.K. carried out and analyzed  
205 all the experiments except the electrophysiology recordings in Figure 3 and Espresso food intake  
206 quantification in Figure 4. E.Z. helped with experiments in Figure 1&2. N.A. helped with experiments  
207 in Figure S2. T. J. wrote the Python code for synchronizing the optogenetic stimulation with video  
208 recordings. N.Y., H.K, M.D., and H.S. designed the electrophysiology experiments in Figure 3 and  
209 Figure S4, which were then carried out and analyzed by H.S. and H.K. The Espresso food intake  
210 experiments in Figure 4 and Figure S3 were carried out and analyzed by X.C and H.K. N.Y. and H.K.  
211 interpreted the results and wrote the paper with feedback from other authors.

### 212 **DECLARATION OF INTERESTS**

213 The authors declare no competing interests.

## MAIN-TEXT FIGURES, FIGURE TITLES, AND LEGENDS



214 **Figure 1. Continuous optogenetic activation of sweet taste neurons leads to gustatory**  
 215 **habituation.**

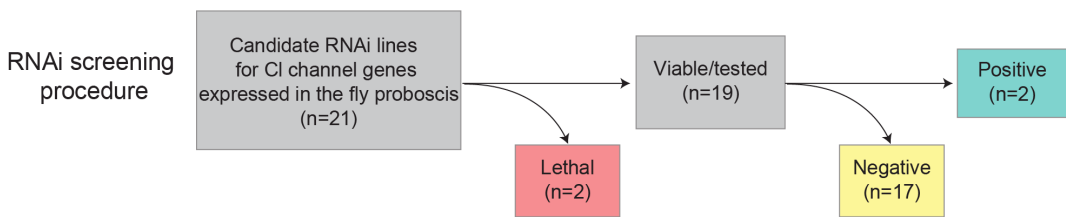
216 (A) Schematic of the optogenetic stimulation and spherical treadmill setup.

217 (B) Representative images for labeled body parts on the fly's head (purple=Head, blue=Rostrum,  
 218 green=Haustellum, and yellow=Labellum) and the rostrum angle ( $\theta$ ).

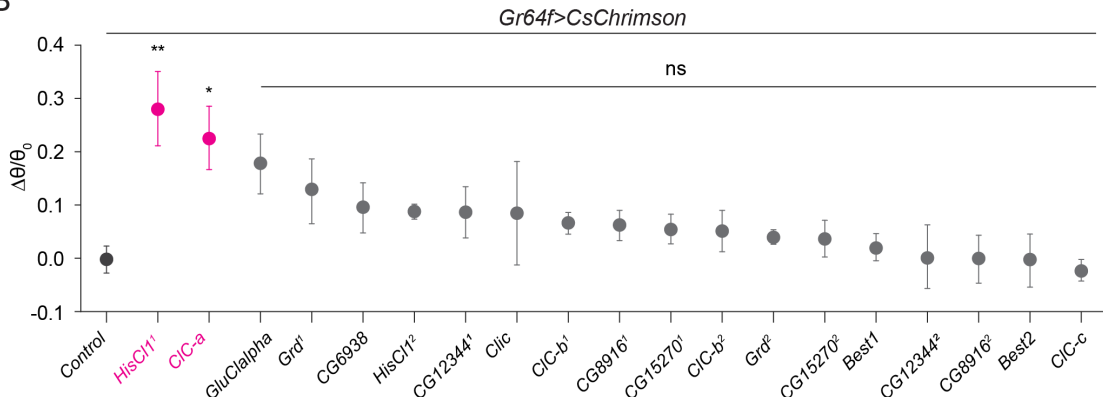
219 (C) Schematic of the DeepLabCut™ pose estimation training process.

220 (D-E) Change in rostrum angle ( $\Delta\theta/\theta_0$ ) is plotted over time (left, mean  $\pm$  SEM) and as a heatmap  
 221 (middle and right) in response to continuous (D) and pulsed (E) optogenetic activation (green=retinal  
 222 fed flies, gray=no retinal controls, n=6-11). Magenta highlights represent when the LED light is ON  
 223 for optogenetic activation. See also Videos S1 and S2.

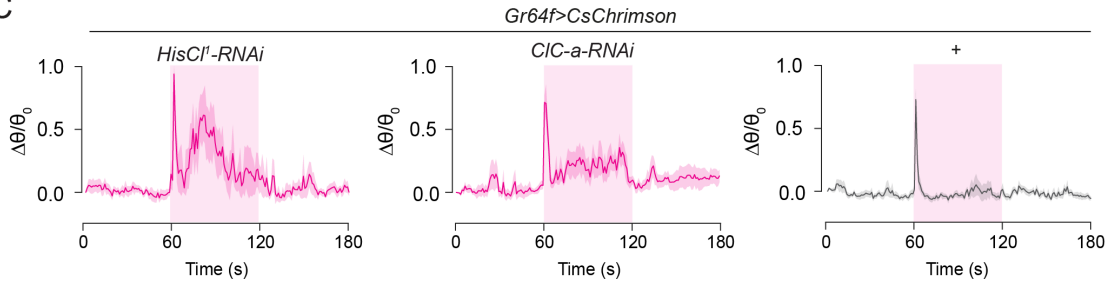
A



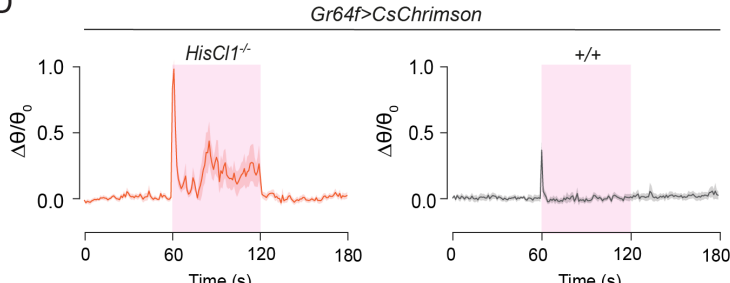
B



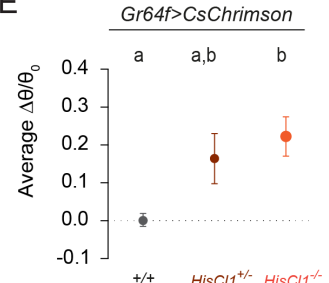
C



D



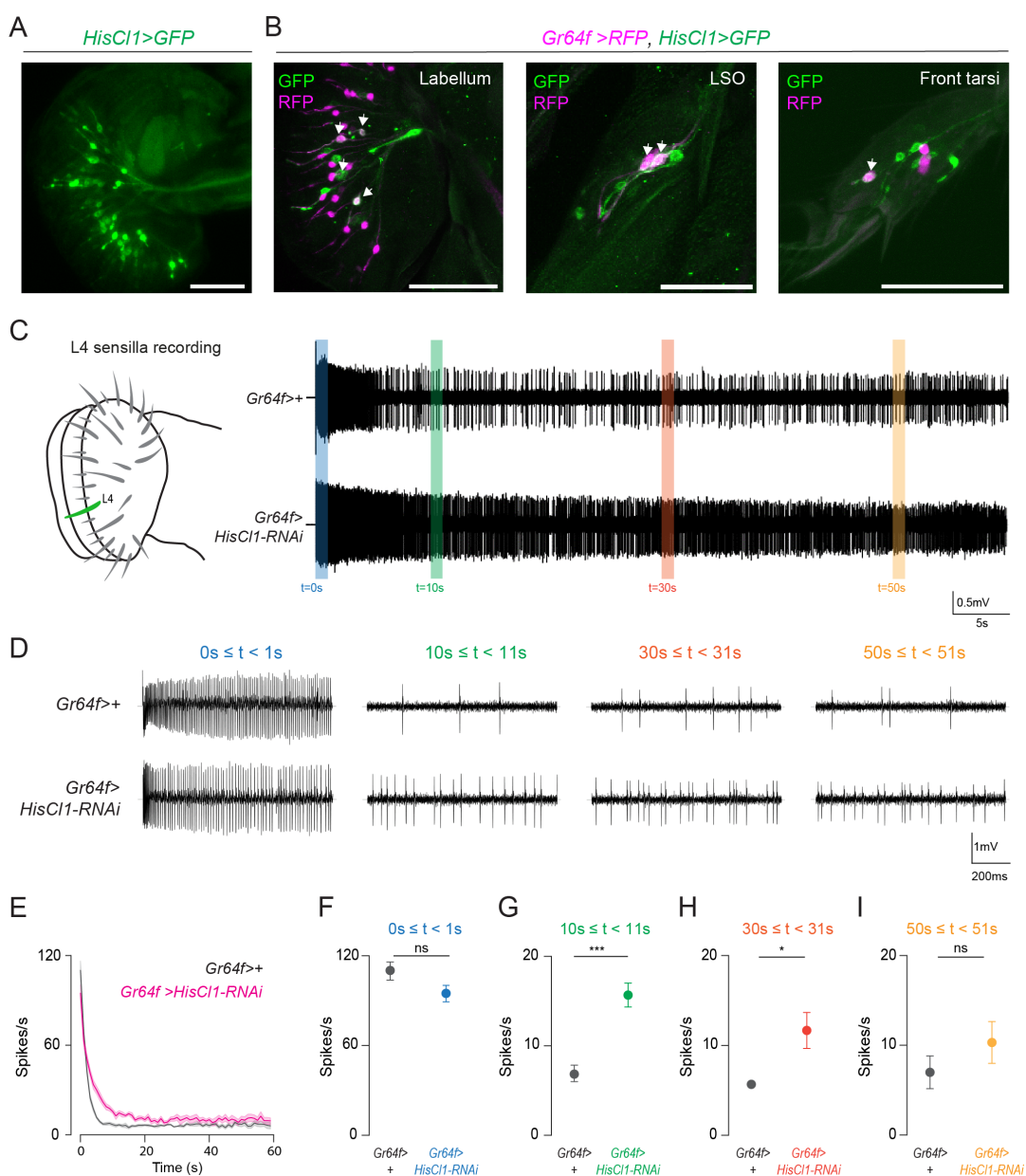
E



224  
225

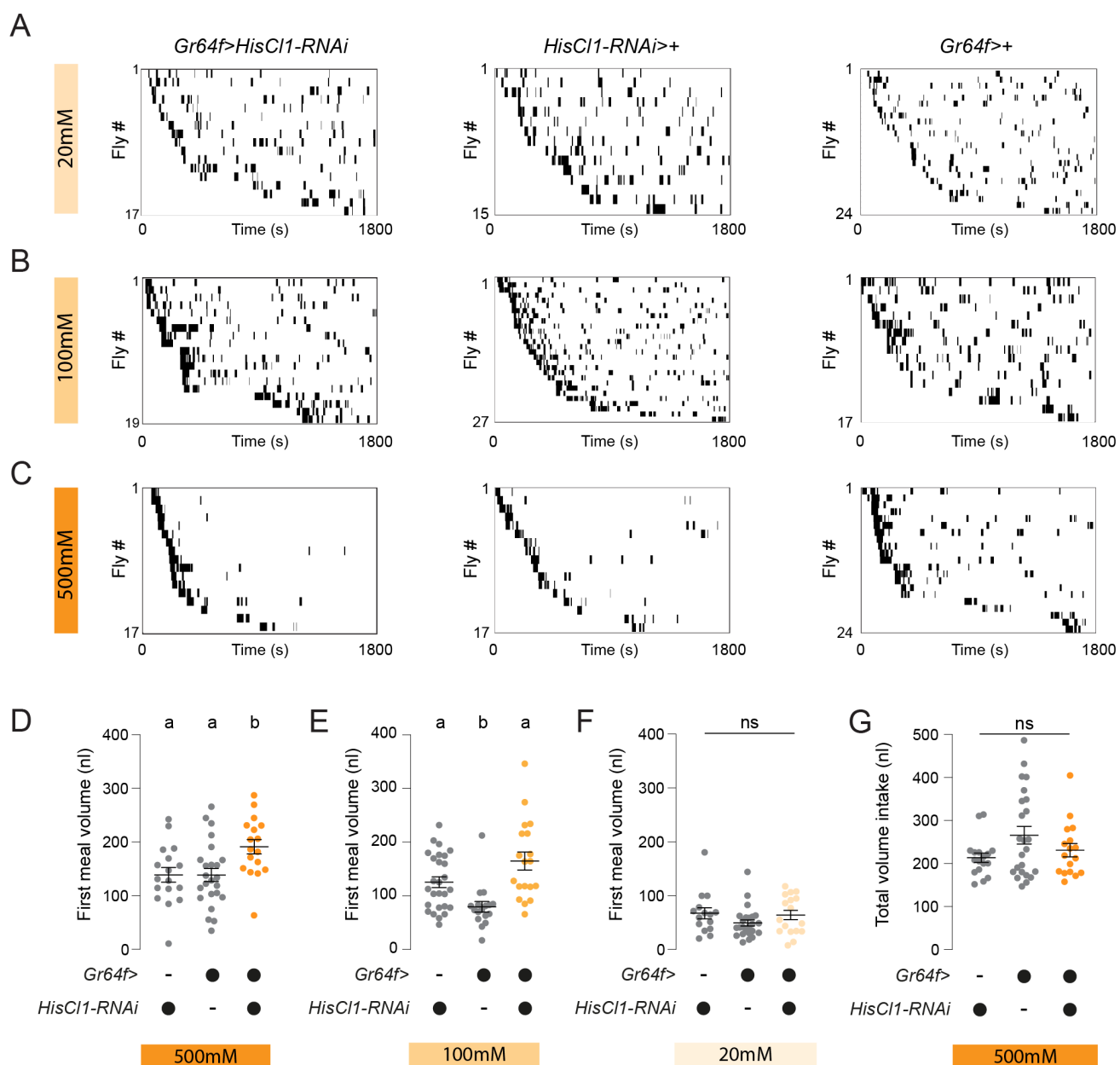
## Figure 2. Knock-down of *HisCl1* and *CIC-a* in sweet taste neurons suppresses gustatory habituation

226 (A) Outline of the transgenic RNAi screening procedure.  
227 (B) Average  $\Delta\theta/\theta_0$  for each RNAi line is quantified and plotted during continuous activation of sweet  
228 taste neurons. Magenta-labeled RNAi lines are significantly different from the control. (n=6-8, one-  
229 way ANOVA with Bonferroni test, \*p<0.05, \*\*p<0.01, ns = non-significant).  
230 (C-D)  $\Delta\theta/\theta_0$  is plotted over time (mean  $\pm$  SEM, n=6-12) for indicated genotypes in response to  
231 continuous optogenetic activation. Magenta highlights represent when the LED light is ON for  
232 optogenetic activation.  
233 (E) Average  $\Delta\theta/\theta_0$  during optogenetic stimulation for *HisCl1*<sup>⁻/⁻</sup> and controls in response to continuous  
234 activation of sweet taste neurons. (n=12, one-way ANOVA with Bonferroni test, genotypes labeled by  
235 different letters are statistically different from each other).  
236 See also Figure S1 and Video S3.



237 **Figure 3. *HisCl1* is expressed in sweet taste neurons and regulates spike frequency adaptation**  
238 **during continuous sugar stimulation in these neurons.**

239 (A) Expression of *HisCl1>* (green) in the labellum (Scale bar=50 $\mu$ m).  
240 (B) Co-labeling of neurons expressing *Gr64f* (magenta) and *HisCl1* (green) in the labellum, LSO,  
241 and front tarsi. White arrows indicate *Gr64*+ and *HisCl1*+ neurons (Scale bars=50 $\mu$ m).  
242 (C) Representative single sensillum recording traces from L4 sensilla of control (top) and  
243 *Gr64f>HisCl1-RNAi* (bottom) flies during a 60-second 500mM sucrose stimulation. Colored vertical  
244 bars indicate time windows for firing rate quantifications in D.  
245 (D) Representative single sensillum recording traces from L4 sensilla of control (top) and  
246 *Gr64f>HisCl1-RNAi* (bottom) flies during 500mM sucrose stimulation in indicated time windows.  
247 (E) Average L4 firing rates of control (gray) and *Gr64f>HisCl1-RNAi* (magenta) flies are plotted over  
248 time (mean  $\pm$  SEM, n=6).  
249 (F-I) Average L4 firing rates of control (gray) and *Gr64f>HisCl1-RNAi* flies in indicated time windows  
250 (0-1s blue, 10-11s green, 30-31s orange, 50-51s yellow). Mean  $\pm$  SEM, n=6, unpaired t-test with  
251 Welch's correction, ns=non-significant, \*p<0.05, \*\*\*p<0.001).



252

**Figure 4. HisCl1 is required in sweet taste neurons to regulate sugar ingestion**

253

(A-C) Meal bout raster plots of 19-23hr food-deprived flies of indicated genotypes ingesting 20mM (A), 100mM (B), or 500mM (C) sucrose solution in the Espresso. The trial duration is 30 minutes (n=15-27, indicated in the y-axis of each plot).

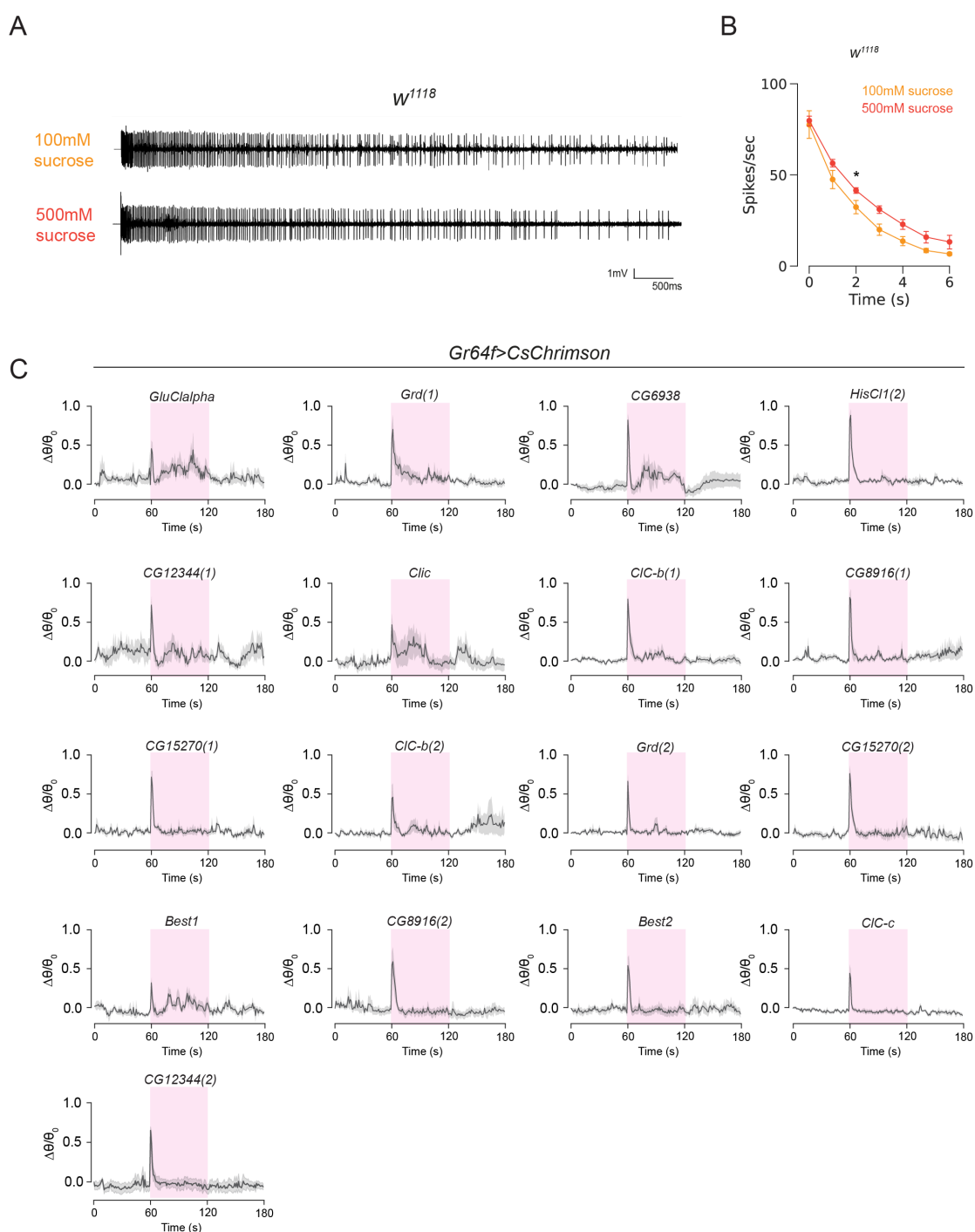
256

(D-F) Average first meal bout volume of flies from indicated genotypes ingesting 500mM (D), 100mM (E), or 20mM (F) sucrose solution in the Espresso (n=15-27, mean  $\pm$  SEM, one-way ANOVA with Bonferroni test. Groups labeled with different letters are significantly different, ns=non-significant).

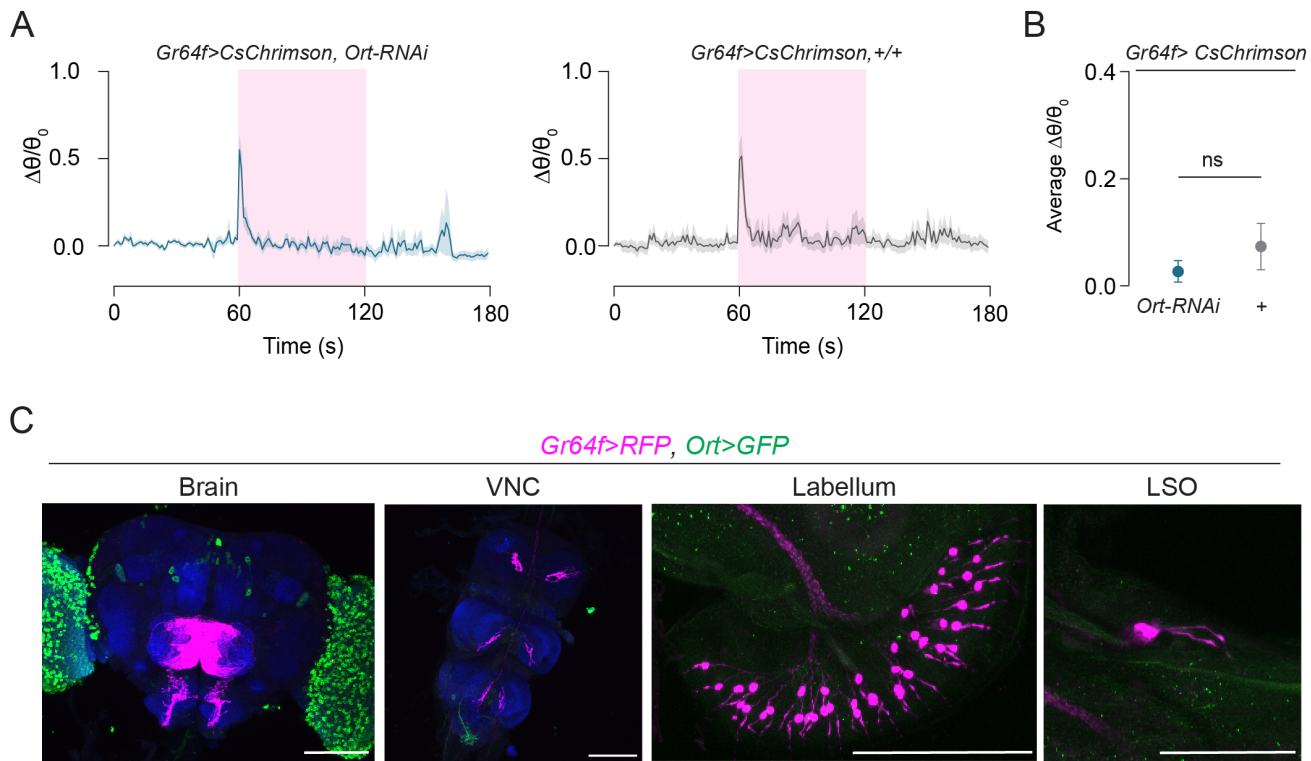
259

(G) The average total volume ingested for flies from indicated genotypes offered 500mM sucrose solution in the Espresso (n=17-24, mean  $\pm$  SEM, one-way ANOVA, ns=non-significant).

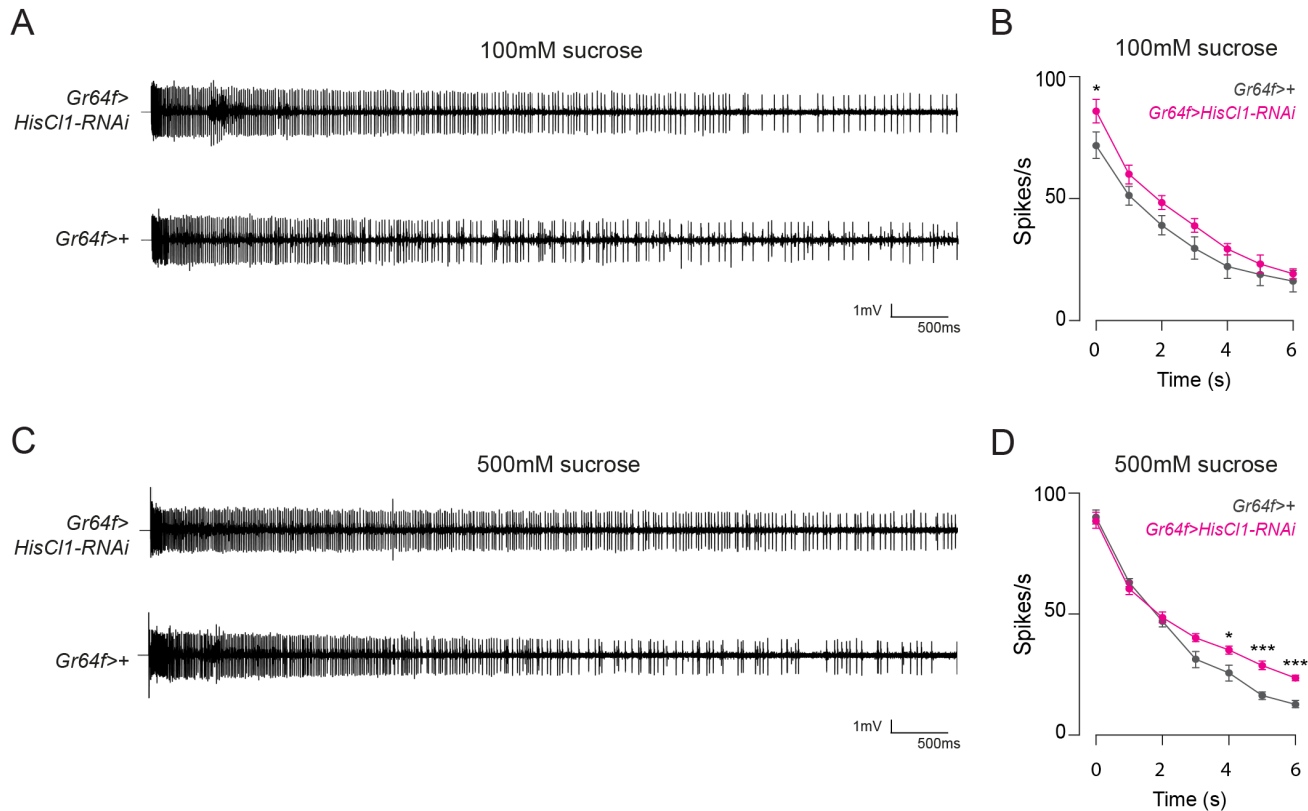
## SUPPLEMENTAL FIGURES, FIGURE TITLES, AND LEGENDS



261 **Figure S1. Single sensillum recording of taste neurons during continuous sugar stimulation**  
262 **and optogenetics data for negative RNAi lines targeting chloride channel genes**  
263 (A) Representative single sensillum recording traces from L4 sensilla of control flies during 100mM  
264 and 500mM sucrose stimulation.  
265 (B) The L4 firing rates during 100mM or 500mM sucrose stimulation are plotted over time (n=6-8,  
266 mean  $\pm$  SEM, two-way ANOVA with Fisher's pairwise comparison, \* p<0.05).  
267 (C)  $\Delta\theta/\theta_0$  is plotted over time (mean  $\pm$  SEM, n=6-8) for indicated genotypes in response to continuous  
268 optogenetic activation. Magenta highlights represent when the LED light is ON for optogenetic  
269 activation.



270 **Figure S2. Knock-down of *Ort* in sweet taste neurons does not affect gustatory habituation.**  
271 (A)  $\Delta\theta/\theta_0$  is plotted over time (mean  $\pm$  SEM, n=6-8) for indicated genotypes in response to continuous  
272 optogenetic activation. Magenta highlights represent when the LED light is ON for optogenetic  
273 activation.  
274 (B) Average  $\Delta\theta/\theta_0$  during optogenetic stimulation for *Ort-RNAi* and control flies in response to  
275 continuous activation of sweet taste neurons (n=6-8, unpaired t-test with Welch's corrections).  
276 (C) Labeling of neurons expressing *Gr64f>* (magenta) and *Ort>* (green) in the brain, VNC, labellum,  
277 and LSO. *Ort>* is expressed in the optic lobes and a few central neurons but not in any of the taste  
278 organs (Scale bars=50 $\mu$ m).



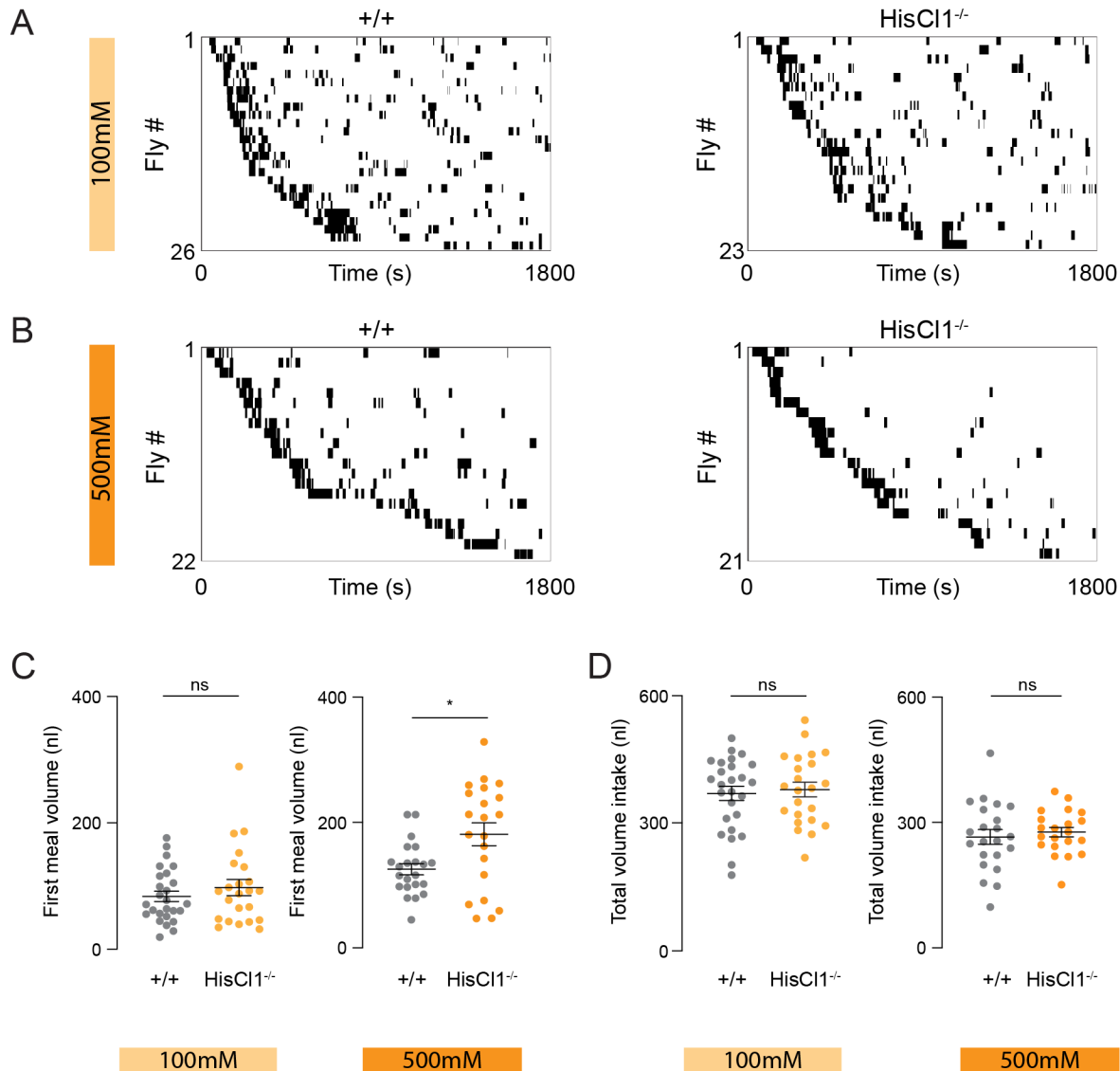
279 **Figure S3. Knock-down of *HisCl1* in sweet taste neurons suppresses spike frequency**  
280 **adaptation during high-concentration sucrose stimulation.**

281 (A) Representative single sensillum recording traces from L4 sensilla of *Gr64f>HisCl1-RNAi* and  
282 control flies during 100mM sucrose stimulation.

283 (B) The L4 firing rates during 100mM sucrose stimulation are plotted over time for indicated genotypes  
284 (mean  $\pm$  SEM, two-way ANOVA with Fisher's pairwise comparison n=6-7).

285 (C) Representative single sensillum recording traces from L4 sensilla of *Gr64f>HisCl1-RNAi* and  
286 control flies during 500mM sucrose stimulation.

287 (D) The L4 firing rates during 500mM sucrose stimulation is plotted over time for indicated genotypes  
288 (mean  $\pm$  SEM, two-way ANOVA with Fisher's pairwise comparison n=6-7).



289 **Figure S4. HisCl1 mutant flies increase their first bout volume while ingesting high-  
290 concentration sugar solution.**

291 (A-B) Meal bout raster plots of 19-23hr food deprived HisCl1 mutant or control flies ingesting 100mM  
292 (A) or 500mM (B) sucrose solution in the Expresso.

293 (C) Average first meal bout volume of HisCl1 mutant or control flies ingesting 100mM, or 500mM  
294 sucrose solution in the Expresso (100mM n=23-26, 500mM n=21-22, mean  $\pm$  SEM unpaired t-test  
295 with Welch's correction, ns=non-significant, \*p<0.05).

296 (D) Average total meal bout volume ingested for HisCl1 mutant, or control flies offered 100mM, or  
297 500mM sucrose solution in the Expresso (100mM n=23-26, 500mM n=21-22, mean  $\pm$  SEM unpaired  
298 t-test with Welch's correction, ns=non-significant, \*p<0.05).

299 **REFERENCES**

300 1. Trisal, S., Aranha, M., Chodankar, A., VijayRaghavan, K., and Ramaswami, M. (2022). A  
301 Drosophila Circuit for Habituation Override. *J Neurosci* 42, 2930-2941.  
302 10.1523/JNEUROSCI.1842-21.2022.

303 2. Paranjpe, P., Rodrigues, V., VijayRaghavan, K., and Ramaswami, M. (2012). Gustatory  
304 habituation in Drosophila relies on rutabaga (adenylate cyclase)-dependent plasticity of  
305 GABAergic inhibitory neurons. *Learn Mem* 19, 627-635. 10.1101/lm.026641.112.

306 3. Inagaki, H.K., Jung, Y., Hooper, E.D., Wong, A.M., Mishra, N., Lin, J.Y., Tsien, R.Y., and  
307 Anderson, D.J. (2014). Optogenetic control of Drosophila using a red-shifted  
308 channelrhodopsin reveals experience-dependent influences on courtship. *Nat Methods* 11,  
309 325-332. 10.1038/nmeth.2765.

310 4. Matsunami, H., and Amrein, H. (2003). Taste and pheromone perception in mammals and  
311 flies. *Genome Biol* 4, 220. 10.1186/gb-2003-4-7-220.

312 5. Yarmolinsky, D.A., Zuker, C.S., and Ryba, N.J. (2009). Common sense about taste: from  
313 mammals to insects. *Cell* 139, 234-244. 10.1016/j.cell.2009.10.001.

314 6. Matsunami, H., and Amrein, H. (2004). Taste perception: how to make a gourmet mouse. *Curr  
315 Biol* 14, R118-120.

316 7. Cobb, M., Scott, K., and Pankratz, M. (2009). Gustation in *Drosophila melanogaster*. *SEB Exp  
317 Biol Ser* 63, 1-38.

318 8. Scott, K. (2018). Gustatory Processing in *Drosophila melanogaster*. *Annu Rev Entomol* 63,  
319 15-30. 10.1146/annurev-ento-020117-043331.

320 9. Clyne, P.J., Warr, C.G., and Carlson, J.R. (2000). Candidate taste receptors in *Drosophila*.  
321 *Science* 287, 1830-1834. 10.1126/science.287.5459.1830.

322 10. Scott, K., Brady, R., Jr., Cravchik, A., Morozov, P., Rzhetsky, A., Zuker, C., and Axel, R.  
323 (2001). A chemosensory gene family encoding candidate gustatory and olfactory receptors in  
324 *Drosophila*. *Cell* 104, 661-673. 10.1016/s0092-8674(01)00263-x.

325 11. Thorne, N., Chromey, C., Bray, S., and Amrein, H. (2004). Taste perception and coding in  
326 *Drosophila*. *Curr Biol* 14, 1065-1079. 10.1016/j.cub.2004.05.019.

327 12. Dunipace, L., Meister, S., McNealy, C., and Amrein, H. (2001). Spatially restricted expression  
328 of candidate taste receptors in the *Drosophila* gustatory system. *Curr Biol* 11, 822-835.  
329 10.1016/s0960-9822(01)00258-5.

330 13. Montell, C. (2009). A taste of the *Drosophila* gustatory receptors. *Curr Opin Neurobiol* 19, 345-  
331 353. 10.1016/j.conb.2009.07.001.

332 14. Gordon, M.D., and Scott, K. (2009). Motor control in a *Drosophila* taste circuit. *Neuron* 61,  
333 373-384. 10.1016/j.neuron.2008.12.033.

334 15. McKellar, C.E., Siwanowicz, I., Dickson, B.J., and Simpson, J.H. (2020). Controlling motor  
335 neurons of every muscle for fly proboscis reaching. *Elife* 9. 10.7554/elife.54978.

336 16. Dahanukar, A., Foster, K., van der Goes van Naters, W.M., and Carlson, J.R. (2001). A Gr  
337 receptor is required for response to the sugar trehalose in taste neurons of *Drosophila*. *Nat  
338 Neurosci* 4, 1182-1186. 10.1038/nn765.

339 17. Dahanukar, A., Lei, Y.T., Kwon, J.Y., and Carlson, J.R. (2007). Two Gr genes underlie sugar  
340 reception in *Drosophila*. *Neuron* 56, 503-516. 10.1016/j.neuron.2007.10.024.

341 18. Inagaki, H.K., Panse, K.M., and Anderson, D.J. (2014). Independent, reciprocal  
342 neuromodulatory control of sweet and bitter taste sensitivity during starvation in *Drosophila*.  
343 *Neuron* 84, 806-820. 10.1016/j.neuron.2014.09.032.

344 19. Inagaki, H.K., Ben-Tabou de-Leon, S., Wong, A.M., Jagadish, S., Ishimoto, H., Barnea, G.,  
345 Kitamoto, T., Axel, R., and Anderson, D.J. (2012). Visualizing neuromodulation *in vivo*:  
346 TANGO-mapping of dopamine signaling reveals appetite control of sugar sensing. *Cell* 148,  
347 583-595. 10.1016/j.cell.2011.12.022.

348 20. May, C.E., Vaziri, A., Lin, Y.Q., Grushko, O., Khabiri, M., Wang, Q.P., Holme, K.J., Pletcher,  
349 S.D., Freddolino, P.L., Neely, G.G., and Dus, M. (2019). High Dietary Sugar Reshapes Sweet  
350 Taste to Promote Feeding Behavior in *Drosophila melanogaster*. *Cell Rep* 27, 1675-1685  
351 e1677. 10.1016/j.celrep.2019.04.027.

352 21. Marella, S., Mann, K., and Scott, K. (2012). Dopaminergic modulation of sucrose acceptance  
353 behavior in *Drosophila*. *Neuron* 73, 941-950. 10.1016/j.neuron.2011.12.032.

354 22. Mathis, A., Manimanna, P., Cury, K.M., Abe, T., Murthy, V.N., Mathis, M.W., and Bethge, M.  
355 (2018). DeepLabCut: markerless pose estimation of user-defined body parts with deep  
356 learning. *Nat Neurosci* 21, 1281-1289. 10.1038/s41593-018-0209-y.

357 23. Ha, G.E., and Cheong, E. (2017). Spike Frequency Adaptation in Neurons of the Central  
358 Nervous System. *Exp Neurobiol* 26, 179-185. 10.5607/en.2017.26.4.179.

359 24. Gengs, C., Leung, H.T., Skingsley, D.R., Iovchev, M.I., Yin, Z., Semenov, E.P., Burg, M.G.,  
360 Hardie, R.C., and Pak, W.L. (2002). The target of *Drosophila* photoreceptor synaptic  
361 transmission is a histamine-gated chloride channel encoded by *ort* (*hclA*). *J Biol Chem* 277,  
362 42113-42120. 10.1074/jbc.M207133200.

363 25. Gisselmann, G., Pusch, H., Hovemann, B.T., and Hatt, H. (2002). Two cDNAs coding for  
364 histamine-gated ion channels in *D. melanogaster*. *Nat Neurosci* 5, 11-12. 10.1038/nn787.

365 26. Zheng, Y., Hirschberg, B., Yuan, J., Wang, A.P., Hunt, D.C., Ludmerer, S.W., Schmatz, D.M.,  
366 and Cully, D.F. (2002). Identification of two novel *Drosophila melanogaster* histamine-gated  
367 chloride channel subunits expressed in the eye. *J Biol Chem* 277, 2000-2005.  
368 10.1074/jbc.M107635200.

369 27. Schnaitmann, C., Haikala, V., Abraham, E., Oberhauser, V., Thestrup, T., Griesbeck, O., and  
370 Reiff, D.F. (2018). Color Processing in the Early Visual System of *Drosophila*. *Cell* 172, 318-  
371 330 e318. 10.1016/j.cell.2017.12.018.

372 28. Jiao, Y., Moon, S.J., Wang, X., Ren, Q., and Montell, C. (2008). Gr64f is required in  
373 combination with other gustatory receptors for sugar detection in *Drosophila*. *Curr Biol* 18,  
374 1797-1801. 10.1016/j.cub.2008.10.009.

375 29. Yapici, N., Cohn, R., Schusterreiter, C., Ruta, V., and Vosshall, L.B. (2016). A Taste Circuit  
376 that Regulates Ingestion by Integrating Food and Hunger Signals. *Cell* 165, 715-729.  
377 10.1016/j.cell.2016.02.061.

378 30. Hartzell, C., Putzier, I., and Arreola, J. (2005). Calcium-activated chloride channels. *Annu Rev  
379 Physiol* 67, 719-758. 10.1146/annurev.physiol.67.032003.154341.

380 31. Taylor, R., and Roper, S. (1994). Ca(2+)-dependent Cl- conductance in taste cells from  
381 *Necturus*. *J Neurophysiol* 72, 475-478. 10.1152/jn.1994.72.1.475.

382 32. Oh, Y., Jang, D., Sonn, J.Y., and Choe, J. (2013). Histamine-HisCl1 receptor axis regulates  
383 wake-promoting signals in *Drosophila melanogaster*. *PLoS One* 8, e68269.  
384 10.1371/journal.pone.0068269.

385 33. Hong, S.T., Bang, S., Paik, D., Kang, J., Hwang, S., Jeon, K., Chun, B., Hyun, S., Lee, Y., and  
386 Kim, J. (2006). Histamine and its receptors modulate temperature-preference behaviors in  
387 *Drosophila*. *J Neurosci* 26, 7245-7256. 10.1523/JNEUROSCI.5426-05.2006.

388 34. Cash, S., Zucker, R.S., and Poo, M.M. (1996). Spread of synaptic depression mediated by  
389 presynaptic cytoplasmic signaling. *Science* 272, 998-1001. 10.1126/science.272.5264.998.

390 35. Tao, H., Zhang, L.I., Bi, G., and Poo, M. (2000). Selective presynaptic propagation of long-  
391 term potentiation in defined neural networks. *J Neurosci* 20, 3233-3243.

392 36. Haberkern, H., Basnak, M.A., Ahanonu, B., Schauder, D., Cohen, J.D., Bolstad, M., Bruns,  
393 C., and Jayaraman, V. (2019). Visually Guided Behavior and Optogenetically Induced  
394 Learning in Head-Fixed Flies Exploring a Virtual Landscape. *Curr Biol* 29, 1647-1659 e1648.  
395 10.1016/j.cub.2019.04.033.

396 37. Moore, R.J., Taylor, G.J., Pault, A.C., Pearson, T., van Swinderen, B., and Srinivasan, M.V.  
397 (2014). FicTrac: a visual method for tracking spherical motion and generating fictive animal  
398 paths. *J Neurosci Methods* 225, 106-119. 10.1016/j.jneumeth.2014.01.010.

399 38. Jeong, Y.T., Oh, S.M., Shim, J., Seo, J.T., Kwon, J.Y., and Moon, S.J. (2016).  
400 Mechanosensory neurons control sweet sensing in *Drosophila*. *Nat Commun* 7, 12872.  
401 10.1038/ncomms12872.

402 39. Delventhal, R., Kiely, A., and Carlson, J.R. (2014). Electrophysiological recording from  
403 *Drosophila* labellar taste sensilla. *J Vis Exp*, e51355. 10.3791/51355.

404 40. Min, S., Oh, Y., Verma, P., Whitehead, S.C., Yapici, N., Van Vactor, D., Suh, G.S., and  
405 Liberles, S. (2021). Control of feeding by Piezo-mediated gut mechanosensation in  
406 *Drosophila*. *Elife* 10. 10.7554/eLife.63049.

407 **STAR METHODS**

408 **RESOURCE AVAILABILITY**

409 **Lead contact**

410 Further information and requests for resources and reagents should be directed to and will be fulfilled  
411 by the lead contact, Nilay Yapici ([ny96@cornell.edu](mailto:ny96@cornell.edu)).

412 **Materials availability**

413 This study did not generate new unique reagents.

414 **Data and code availability**

415 The data supporting this study's findings are available from the lead contact upon reasonable  
416 request.

417 This study did not generate new code.

418 Any additional information required to reanalyze the data reported in this paper is available from  
419 the lead contact upon reasonable request.

420

421 **EXPERIMENTAL MODEL AND SUBJECT DETAILS**

422 **Flies**

423 *Drosophila melanogaster* was maintained on conventional cornmeal-agar-molasses medium at 25°C  
424 and 60-70% relative humidity under a 12hr light: 12hr dark cycle (lights on at 9 A.M.). Fly stocks and  
425 genotypes are detailed in Key Resources and Table S1. All fly stocks were obtained from Bloomington  
426 Drosophila Stock Center unless otherwise stated. The candidate genes targeted in the screen were  
427 selected for their functional annotation as Cl<sup>-</sup> channels and their expression in the fly proboscis based  
428 on previous RNA sequencing experiments <sup>20</sup>.

429

430 **METHOD DETAILS**

431 **Optogenetic activation on the spherical treadmill**

432 6–10-day old male flies were used in all optogenetic activation experiments. All flies were food  
433 deprived for 18–24 hours. During deprivation, test group flies were kept in a vial containing a Kimwipe  
434 (Kimtech Science™) soaked with 0.5mM all-trans-retinal (Sigma, R2500), and control flies were kept  
435 with a Kimwipe soaked with water. The spherical treadmill was custom-built from polyurethane foam  
436 (FR-7112, Last-A-Foam, General Plastics Manufacturing Company), as previously described <sup>36</sup>. The  
437 ball had a 10mm diameter and a weight of 97mg, and it was air-floated by an air pump attached to a  
438 mass flow controller working at 0.45l/min. Two IR LED lights were used to illuminate the ball and the  
439 fly for better tracking quality (SZ-01-R8, Luxeon Star). The humidity of the air was maintained by  
440 passing it through a bottle humidifier (Salter Labs). During the optogenetic activation experiments,  
441 flies were tethered but allowed to walk on a spherical treadmill in the dark. Each trial started with a  
442 60s recording of fly behavior without optogenetic stimulation, followed by 60s optogenetic stimulation,  
443 and another 60s recording without stimulation. The 625nm red LED light (Thorlabs, M625F2) was

444 powered at 14 $\mu$ W/mm<sup>2</sup> using a LED driver (Thorlabs, LEDD1B). During the optogenetic stimulation  
445 experiments, the red light was delivered to the fly using an optic fiber cannula (Thorlabs, CFMC22L20)  
446 (Figure 1). We used two optogenetic stimulation patterns; continuous activation (total duration=60s,  
447 LED constantly ON) and pulse activation (total duration=60s, LED 0.1Hz,100ms ON, 9900ms OFF).  
448 During the experiments, the movement of the fly's proboscis was recorded using a Blackfly-S camera  
449 (BFS-U3-13Y3M-C, FLIR), and the fly/ball movements were recorded using a Firefly camera (FMVU-  
450 03MTM-CS, FLIR). All videos were acquired at 30fps. A custom-written script in Python controlled all  
451 video recordings and optogenetic stimulation patterns. We used FicTrac software <sup>37</sup> to extract the fly  
452 locomotion data by tracking the ball's movements.

#### 453 **Transgenic RNAi screen**

454 Each transgenic RNAi line was crossed to flies carrying *Gr64f-GAL4* and *UAS-CsChrimson-mCherry*.  
455 To generate control flies, we crossed flies carrying *Gr64f-GAL4* and *UAS-CsChrimson-mCherry* to  
456 *w<sup>1118</sup>*. 6–10-day old male flies from the progeny were tested in the optogenetic activation experiments.  
457 All flies tested were food deprived for 24 hours in a vial containing a Kimwipe (Kimtech Science™)  
458 soaked with 0.5mM all-trans-retinal.

#### 459 **Expresso Food Intake Quantification**

460 Flies tested in the Expresso assay were prepared as described before <sup>29</sup>. Briefly, 6–10-day old male  
461 flies were food deprived for 19–24 hours in a fly vial containing a piece of Kimwipe (Kimtech  
462 Science™) soaked with 1ml MilliQ water. On the day of the experiment, sucrose (Sigma, S5390)  
463 solutions were freshly prepared. Each fly was placed into a test cuvette and allowed to habituate for  
464 5–10 mins before the start of the trial. Each trial lasted 30 mins, and the food intake data was recorded  
465 using the Expresso data acquisition software <sup>29</sup>.

#### 466 **Immunohistochemistry and Confocal Microscopy**

467 Brain immunohistochemistry was carried out as previously described <sup>29</sup> with minor modifications. First,  
468 brains were dissected and fixed for 25 min with 4% paraformaldehyde (PFA) in PBST (PBS+0.3%  
469 Triton-X). After washing with PBST (4 times, 15 mins each), they were incubated with the blocking  
470 solution (5% normal goat serum (NGS, Jackson Labs, 005-000-121) in PBST) for 1.5 hours. Next,  
471 brains were incubated with the primary antibodies for two days at 4°C. After washing with PBST (3  
472 times, 30 mins each), brains were incubated with the secondary antibodies for two days at 4°C.  
473 Finally, samples were mounted with SlowFade™ Gold Antifade Mountant (Thermo Fisher Scientific,  
474 S36936). Proboscis immunohistochemistry was carried out as previously described <sup>38</sup> with minor  
475 modifications. Proboscises were dissected and fixed with 4% PFA in PBST. After washing with PBST,  
476 samples were incubated with the blocking solution for 1.5 hours. Next, they were incubated with the  
477 primary antibodies for two days at 4°C. After washing with PBST (3 times, 30 min each), samples  
478 were incubated with the secondary antibodies for two days at 4°C. Samples were mounted with

479 SlowFade™ Gold Antifade Mountant (Thermo Fisher Scientific, S36936). For imaging tarsi, legs were  
480 dissected and fixed with 4% PFA in PBST. After washing with PBST (3 times, 30 mins each), legs  
481 were mounted with SlowFade™ Gold Antifade Mountant (Thermo Fisher Scientific, S36936).  
482 Following antibodies were used for the immunohistochemistry: chicken anti-GFP (1:2000, Abcam,  
483 ab13970), rabbit anti-DsRed (1:500, Takara Bio, 632496), and mouse anti-Brp (1:20, DSHB, nc82),  
484 goat anti-chicken Alexa 488 (1:1000, Invitrogen, A-11039), goat anti-rabbit Alexa 546 (1:500,  
485 Invitrogen, A-11035), and goat anti-mouse Alexa 633 (1:500, Invitrogen, A-21052). All images were  
486 acquired using a Zeiss Confocal microscope (LSM 880) equipped with a 20X water immersion  
487 objective (Nikon, W Plan-Apochromat 20x/1.0). Confocal images were processed using the FIJI  
488 software.

489 **Single Sensillum Electrophysiology**

490 We used the extracellular tip recording method to capture sucrose responses from the labellar taste  
491 sensilla as previously described <sup>39</sup>. 6-10-day-old male flies were cold anesthetized, and the proboscis  
492 was immobilized by inserting the reference electrode containing the Beadle-Ephrussi Ringer solution  
493 through the thorax into the labellum. The neuronal firing rates of the L4 sensilla were recorded using  
494 a glass electrode (10-20  $\mu$ m diameter) containing 100mM or 500mM sucrose mixed with an electrolyte  
495 (30 mM tricholine). The glass recording electrode was connected to the TastePROBE (Syntech) and  
496 the IDAC acquisition controller (Syntech). The signals were amplified (10x), band-pass-filtered (99-  
497 3000 Hz), and sampled at 12 kHz.

498

499 **QUANTIFICATION AND STATISTICAL ANALYSIS**

500 **Proboscis Movement Quantification**

501 The DeepLabCut software <sup>22</sup> was used to track the movements of the proboscis. The pose estimation  
502 model was trained by labeling the coordinates of four body parts on the fly's head (head, rostrum,  
503 haustellum, and labellum) in each video frame. For the training process, we used 1266 frames to  
504 create training datasets. After the first round of training, the network was evaluated for errors by  
505 quantifying the pixel distance between the observed and estimated coordinates. The frames with  
506 errors were corrected and merged into the original training dataset, and the network was re-trained.  
507 After all the training, the final average error distance was less than 5 pixels. We used a custom-written  
508 script in Python for data analysis to calculate the rostrum angle ( $\theta$ ) using the three coordinates: head  
509 ( $x_{hd}$ ,  $y_{hd}$ ), rostrum ( $x_r$ ,  $y_r$ ), and haustellum ( $x_h$ ,  $y_h$ ). Python script read all the output files from  
510 DeepLabCut as raw data, and the script collected three coordinates to compute the rostrum angle.  
511 Using three coordinates, two vectors were generated:  $\overrightarrow{RHd}$  (head-rostrum) and  $\overrightarrow{RH}$  (rostrum-  
512 haustellum). To calculate the angle between the two vectors, we used the atan2 function that  
513 computes the counterclockwise angle between two vectors. Each rostrum angle was then averaged  
514 and aggregated in seconds. We calculated the  $\Delta\theta/\theta_0$  for all flies tested using the following formula,

515  $\frac{\Delta\theta}{\theta_0} = \frac{\theta_t - \theta_0}{\theta_0}$  ( $\theta_0$ = initial angle t=0),  $\theta_t$ = angle at time (t),  $\Delta\theta = \theta_t - \theta_0$ ). Average  $\Delta\theta/\theta_0$  was calculated by  
516 averaging all values during the stimulation period (t=60-120s).

517 **Electrophysiology Data Analysis**

518 To analyze neuronal firing rates in response to sugar stimulation, spikes were sorted manually, then  
519 the number of spikes per stimulation was determined using the Autospike software. Next, the total  
520 number of spikes was binned per second and plotted as a time series for each genotype. To quantify  
521 how neuronal firing rates changed between the early and the late phases of the recordings, average  
522 firing rates per genotype were calculated for the following time windows: short recordings  
523 (duration=6s);  $0s \leq t < 3s$  and  $4s \leq t < 7s$ , and long recordings (duration=60s);  $0s \leq t < 1s$ ,  $10s \leq t <$   
524  $11s$ ,  $30s \leq t < 31s$ , and  $50s \leq t < 51s$ ). The average spike rates in each time window were compared  
525 between the controls and *Gr64f>HisC11* knock-down flies using the GraphPad Prism software.

526 **Expresso Food Intake Analysis**

527 We used a custom-written code to analyze the Expresso food intake data <sup>40</sup>. Each automatically  
528 detected meal bout was manually checked, and if there were mislabeled eating meal bouts in a trial,  
529 those flies were excluded from the data set. These mislabeled trials were less than ~14% of total  
530 trials. We calculated the average total food intake and first meal bout volume of flies that have taken  
531 at least one meal bout during the assay period. Flies that did not consume food were not included in  
532 the quantifications. Data were plotted as scatter plots, indicating the mean  $\pm$  SEM. Statistical analyses  
533 were performed using GraphPad Prism software.